ISBN: 978-3-95450-236-3 ISSN: 2673-5350 doi:10.18429/JACoW-IBIC2023-TUP034

AXIAL CRYOGENIC CURRENT COMPARATOR (CCC) FOR FAIR

L. Crescimbeni†[1,], F. Schmid[1], Friedrich-Schiller-University Jena, Jena, Germany
D. M. Haider, A. Reiter, M. Schwickert, T. Sieber
GSI Helmholtz Centre for Heavy Ion Research, Darmstadt, Germany
M. Schmelz, R. Stolz[3], V. Zakosarenko[4], Leibniz IPHT, Jena, Germany
T. Stoehlker[1,2], V. Tympel[1], Helmholtz Institute Jena, Jena, Germany
[1]also at GSI Helmholtz Centre for Heavy Ion Research, Darmstadt, Germany
[2]also at Institute for Optics and Quantum Electronics, Jena, Germany
[3]also at Technical University Ilmenau, Ilmenau, Germany
[4]also at supracon AG, Jena, Germany

Abstract

The Cryogenic Current Comparator (CCC) is a superconducting device based on an ultrasensitive SQUID (superconductive quantum interference device) magnetometer (fT range). Measuring the beam azimuthal magnetic field, it provides a calibrated non-destructive measurement of beam current with a resolution of 10 nA or better, independent from ion species and without tedious calibrations procedure. The non-interceptive absolute intensity measurement of weak ion beams (< 1 μA) is essential in heavy ion storage rings and in transfer lines at FAIR. With standard diagnostics, this measurement is challenging for bunched beams and virtually impossible for coasting beams. To improve the performance of the CCC detector several upgrades are under study and development: One is the investigation of a new type of CCC using an alternative magnetic shield geometry. The so-called "axial" geometry will allow for much higher magnetic shielding factor, an increased pick-up area, and a reduced low frequencies noise component. Further improvements and optimizations of the detector will be presented. The CCC will be tested on the beamline at the end of 2023 allowing to define the best possible version for FAIR.

INTRODUCTION

After proof of principle with an earlier CCC version [1], the first prototype of CCC for GSI and FAIR is the FAIR-Nb-CCC-xD (Fig. 1) that is part of the family of CCC-XD that has been developed for the use with the beamline dimensions at FAIR HEBT (Ø 150 mm).

The CCC is installed in a beam-line cryostat [2] equipped with a helium reliquifier¶ that provides stable operating conditions.

The CCC has been tested in CRYRING@ESR [3] confirming the viability of the detector and its current resolution in the order of nA. The test in CRYRING@ESR has shown some limitation of the system like the limited slew rate and the low magnetic shielding. The CCC prototype is built out of niobium, causing high costs and several mechanical difficulties in the construction process (for example the needing of electron beam wielding). Other than this, the FAIR-Nb-CCC-xD is equipped with a high permeability core, that produces low frequencies noise (due to trapped magnetic field) and introduces the need of a low pass circuit to avoid resonances, reducing the maximum bandwidth of the system.

To improve these aspects of the detector a new version of the CCC, with an axial geometry, has been developed.

NEW AXIAL CORELESS CCC

A new type of CCC, developed together with IPHT Jena, will be built out of lead with an axial shield geometry and without a high permeability core (Fig. 1).

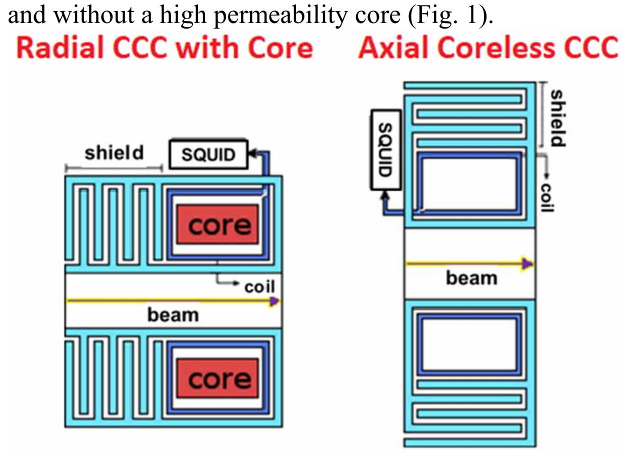

Figure 1: Left: Radial Geometry, like the FAIR-Nb-CCC-xD, with high permeability core. Right: Axial geometry coreless CCC, made of lead, the pickup coil is filled only with non magnetic foam for structural support.

The axial CCC is expected to be less sensitive to external perturbations, in particular very low-frequency noise (<1 Hz), caused by magnetic field caught inside the core material [4], and less sensitive to mechanical perturbation.

The new coreless lead CCC will have a much higher screening factor due to the axial magnetic shield composed of 10 layers of lead sheet [5]. The simulation shows a theoretical screening factor higher than 200 dB, reducing the effect of a magnetic perturbation in the order of 10 μT

*Work supported by AVA – Accelerators Validating Antimatter the EU H2020 Marie-Curie Action No. 721559 and by the BMBF under contract No 05P21SJRB1.
†l.crescimbeni@gsi.de
¶Model PT415 from Cryomech Inc, Syracuse, NY, USA

ISBN: 978-3-95450-236-3 ISSN: 2673-5350 doi:10.18429/JACoW-IBIC2023-TUP034

(amplitude similar to the dipole ramp perturbation observed with the CCC at CRYRING@ESR) to a level below detection threshold of the detector.

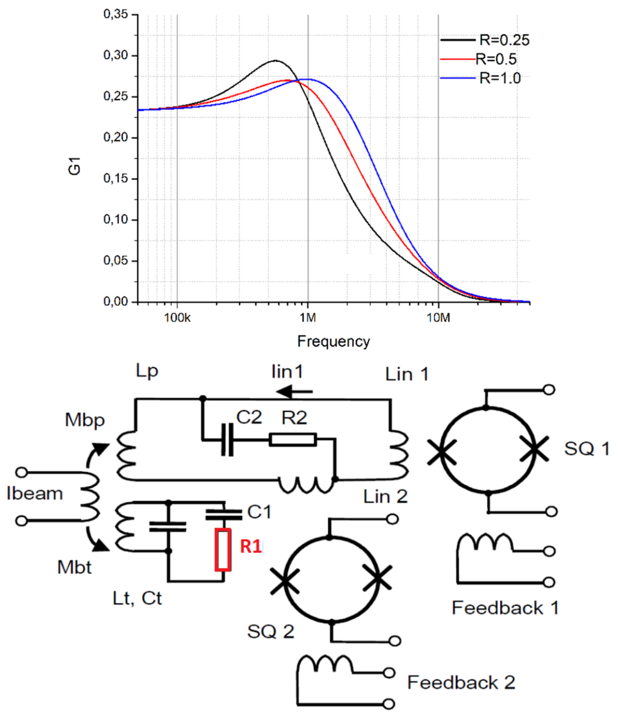

Figure 2: Simulations of the transfer function for CN4 SQUID and schematic of the two parallel squid system. Upper: CN4 squid transfer function. Lower: Circuit Schematic, can be seen the two squids and their feedback system, the damping circuit has been added to avoid resonance peaks in the frequency of interest. The chosen value for the resistance is 0.5 Ohm, to provide the smoothest gain without decreasing the bandwidth.

The improved screening factor, together with the expected lower sensitivity to low-frequency perturbation should increase the sensitivity of the detector in the accelerator environment. This new CCC will be equipped with a parallel SQUID system (Fig. 2), a sensitive SQUID with a lower bandwidth (type CN4, Leibniz IPHT/supracon AG) and a higher bandwidth SQUID with lower sensitivity (type CN2, same provider).

The parallel use of two SQUIDs refers to the introduced cascade principle [6]. The two parallel SQUID system, thanks to the higher bandwidth, will allow to sensibly improve the slew rate of the detector without introducing additional filtering elements, so without decreasing the resolution due to additional thermal noise, (as it was done for the FAIR-Nb-CCC-xD in CRYRING [3]).

PROTOTYPE CONSTRUCTION

The first prototype of the axial coreless CCC has been built in collaboration with IPHT Jena (Fig. 3).

The first part that has been built were the 10 layers meander structure, composing the magnetic shielding. The external meander is built out of a 1 mm pb sheet, placed on the inside of a 250 mm radius fiberglass cylinder to provide structural integrity. The internal structure of 9 meanders are instead built out of 0.25 mm thick Pb-Sl sheet, overlapped with thin electric-insulation layers. The meander structure is then connected to the upper and lower surface of the CCC, built out of 1.5 mm Pb sheets.

At the end of the meander structure the pickup-coil has been built up, in this process two coils of 0.25 mm thickness Pb-Sl sheet are wrapped around a structure composed of XPS Polystyrene foam to provide the required stabilization.

The meanders and the pickup coil are then enclosed in a fiberglass cylinder of 320 mm to provide rigidity to the system and protect it from deformation due to handling during test and installation. The structure is then completed with a last layer of 1 mm Pb sheet that connects the upper and the lower extremity of the CCC.

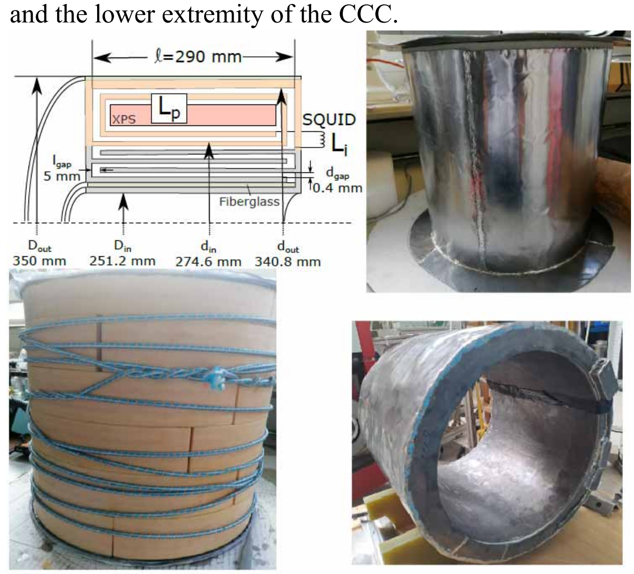

Figure 3: Construction steps of axial CCC. Up left: Scheme of axial CCC. Up right: First meander of the meander structure, the fiberglass cylinder can be seen on the upper part. Down Left: XPS support structure for the pickup coils during assembly. Down Right: Axial lead CCC completed, on the upper corner it's also possible to see the squid box.

The Pickup coil is finally connected through two Pb strips to the squid box installed on top of the CCC. The Pb box in which the SQUIDs are enclosed is necessary to shield them from external magnetic fields.

All the soldering has been performed with Pb-Sn material, to make sure that also the soldering connection are superconductive, and the insulant is kept in place by cryoglue.

FIRST TEST OF AXIAL CORELESS CCC

The Axial CCC has first been tested in the laboratory at FSU Jena (Fig. 4). This test has allowed us to measure the performance of the detector in a controlled environment. The following measurement steps have been performed to stepwise characterize the properties of the axial CCC:

ISBN: 978-3-95450-236-3 ISSN: 2673-5350 doi:10.18429/JACoW-IBIC2023-TUP034

Figure 4: Left: FSU Jena Laboratory with wide-neck cryostat. Right: Axial coreless CCC during installation, the squid box and the cabling is also visible on the top of the CCC. The white windings on the cryostat are the Helmholtz coils for the magnetic shield test. The CCC is at rest in the bottom part of the cryostat.

Current resolution: Using the calibration line of the cryostat it was possible to estimate the current resolution of the system, around 10 nA (Fig. 5).

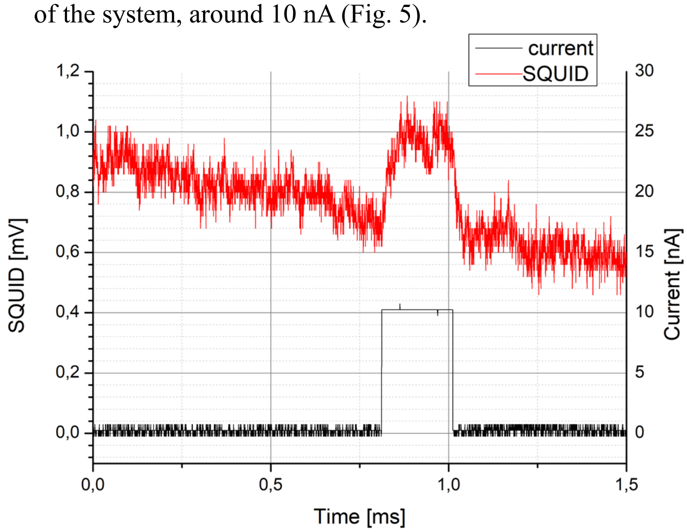

Figure 5: Current resolution of CN4 squid: The black waveform is the rectangular waveform used as input, the red waveform is the squid signal. Maximum current resolution is around 10 nA, lower signal can't be distinguished over the noise floor.

There are two main reason for this low current resolution compared to classical CCC [1 nA]:

- Less coupling of the pickup to the magnetic field of the beam due to the lack of the high permeability core
- Higher noise component at higher frequencies, the noise floor measured with the axial CCC (around 5-10 nA) is unexpectedly more than ten times higher than the noise floor measured in the lab with radial core CCCs, because of low-pass filtering, which is not present in the axial CCC. The low-pass filter is required to avoid resonances, due to the high magnetic permeability core inductance, that together with the capacity of the magnetic shield meander structure behave as an LC circuit. In the coreless CCC the inductance of the pickup coil is much lower, so the low-pass filter is not needed. The resonance frequency of the system is much higher than the maximum bandwidth of the used squids.

Slew Rate: A first estimation of the slew rate has been performed in the cryostat in Jena, estimating the value at around 4 µA/µS, a strong improvement from the 0.16 µA/µS of the FAIR-nB-CCC-xD [3]. It will be possible to reach higher slew rates with further optimization of the hardware (like squid cabling) or of the squid circuit. This will allow to use the CCC for monitoring a higher spectrum of signals without decreasing the current resolution.

Magnetic Shielding: The FSU cryostat is equipped with a pair of Helmholtz coils (Fig. 4) to provide a magnetic field up to 1 mT. The previous test of the FAIR-Nb-CCC-xD has shown a quite high sensitivity to external magnetic field. In CRYRING@ESR the dipole field (~100 µT) produced a signal from the SQUID in the order of 10 nA. For the axial CCC we were not able to detect any squid response to the external magnetic field of 1 mT. Only using a waveform generator to drive the Helmholtz coil we were able to distinguish a small response in the frequency spectrum of the noise, estimating a SQUID signal lower than 0.1 nA. This result doesn't allow to calculate the exact screening factor of the axial CCC or even to verify a theoretical value of ~200 dB (which is anyway not feasible), but it is good enough to confirm that the new shield geometry strongly improves the magnetic screening factor, effectively removing external magnetic fields from the CCC signal.

TEST OF AXIAL CCC IN THE BEAM-LINE CRYOSTAT AT GSI

We proceeded to install the axial CCC in the beam-line cryostat in GSI (Fig. 6). Even if the test in the well shielded laboratory Jena was successful, the high noise component we found there has arisen some worries, which unfortunately found confirmation in the test.

The sensitive squid has shown a very unstable V-ϕ characteristic (Fig. 7), obtained by applying a well defined signal to a coil wound around the SQUID or to the calibration line. This produces a 'calibration' field that is used to obtain the modulation of the squid (in Volt) as a function of the applied field (ϕ).

The working point of the squid in the Flux Looked Loop (FLL) mode is set where the characteristic curve crosses the zero voltage line. To have a stable working point that allows to use the squid in the FLL mode, which is essential for the data acquisition, the characteristic curve

ISBN: 978-3-95450-236-3 ISSN: 2673-5350 doi:10.18429/JACoW-IBIC2023-TUP034

should cross the zero line in a definite point. If the characteristic curve is not stable due to excessive noise, like at our measurement shown in Fig. 6, it is impossible to define a stable working point for the squid.

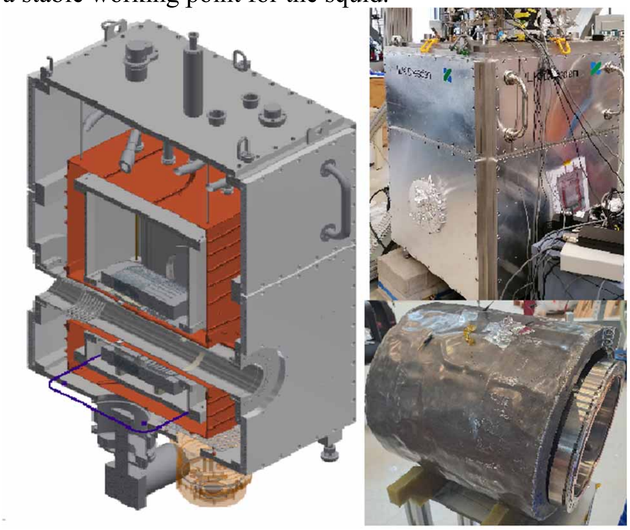

Figure 6: GSI setup, left: cryostat scheme, upper right: cryostat vacuum vessel, lower right: picture of the CCC during installation. The CCC is installed over the He-container tube, the thermal shield tube and finally the UHV tube of the beamline.

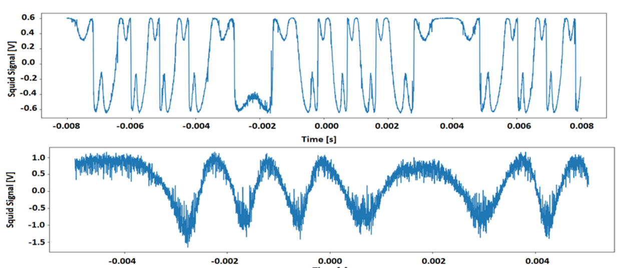

Figure 7: Upper: Squid characteristics in the laboratory in Jena. Lower: Squid characteristic at GSI cryostat. It's possible to see how the characteristic has a deformed shape in respect to the optimal one measured in Jena, moreover the noise has in some points almost half of the full amplitude of the characteristic curve. With a noise component so high the characteristic is very unstable and it's not possible to find a stable working point

The test at GSI has shown that the axial coreless CCC is currently not a valid detector for installation in the beamline cryostat. The absence of a stable working point makes it impossible to perform beam measurement with the CCC.

It was only possible to use the low sensitivity SQUID, that can work independently of the FLL mode, to collect information on the noise (estimated to be higher than 1 µA, around 50 times higher than the noise floor of the classical radial CCC with core). Further investigations will mainly use the low sensitivity SQUID to get a better understanding how the noise couples that strongly to axial coreless CCC and also why the noise is much higher than expected.

CONCLUSION AND NEXT STEPS

The test of the axial coreless CCC has highlighted the issues of the prototype, in particular the low coupling with the beam field due to the lack of the core that together with the high noise floor level, especially at higher frequencies, make the prototype not able to work in the accelerator environment. The test at FSU Jena laboratory has, however, confirmed the validity of the axial magnetic shielding and the effectiveness of the squid cascade system to improve the slew-rate of the detector.

Even if it is confirmed that the axial coreless CCC will not be the solution for FAIR, we are able to use the information achieved on the effectiveness of the axial geometry and the squid cascade system to develop a new prototype of CCC of axial geometry, the Double Core axial CCC, inspired on the design of the CCC Sm (Smart & small) [7].

At the end of 2023 the FAIR-nB-CCC-xD will be tested on the beam line at GSI, allowing us to perform a final test of the cryostat and of the detector on the transfer lines, as they will be used in FAIR. In the first half of 2024 we will test the first prototype of the double core axial CCC in the laboratory, followed by a beamline test in summer 2024.

REFERENCES

[1] A. Peters *et al.,* "A Cryogenic Current Comparator for the absolute Measurement of nA Beams", *AIP Conf. Proc. 451*, pp.163-180, 1998.

[2] D. M. Haider *et al.*, "Versatile Beamline Cryostat for the Cryogenic Current Comparator (CCC) for FAIR", in *Proc. IBIC'19*, Malmö, Sweden, Sep. 2019, pp. 78-81. doi:10.18429/JACoW-IBIC2019-MOPP007

[3] L. Crescimbeni *et al.*, "The Cryogenic Current Comparator at CRYRING@ESR", in *Proc. IBIC'22*, Kraków, Poland, Sep. 2022, pp. 300-303. doi:10.18429/JACoW-IBIC2022-TUP31

[4] V. Zakosarenko *et al.*, "Coreless SQUID-based cryogenic current comparator for non-destructive intensity diagnostics of charged particle beams", *Supercond. Sci. Technol.*, vol. 32, p. 014002, 2018. doi:10.1088/1361-6668/aaf206

[5] H. De Gersem, N. Marsic *et al.*, "Finite-element simulation of the performance of a superconducting meander structure shielding for a cryogenic current comparator*", Nucl. Instrum. Methods Phys. Res. Sect. A,* vol. 840, pp. 77–86, 2016. doi:10.1016/j.nima.2016.10.003

[6] T. Schönau and M. Schmelz, *et al.*, "SQUID-based setup for the absolute measurement of the Earth's magnetic field", *Supercond. Sci. Technol.*, vol. 26, number 3, p. 035013, 2013. doi:10.1088/0953-2048/26/3/035013

[7] V. Tympel *et al.*, "Creation of the First High-Inductance Sensor of the New CCC-Sm Series", in *Proc. IBIC'22*, Kraków, Poland, Sep. 2022, pp. 469-472. doi:10.18429/JACoW-IBIC2022-WEP30